

Measuring silver nanoparticle dissolution in complex biological and environmental matrices using UV–visible absorbance

Justin M. Zook · Stephen E. Long · Danielle Cleveland · Carly Lay A. Geronimo · Robert I. MacCuspie

Received: 27 May 2011 / Revised: 11 July 2011 / Accepted: 15 July 2011 / Published online: 2 August 2011
© Springer-Verlag (outside the USA) 2011

Abstract Distinguishing the toxic effects of nanoparticles (NPs) themselves from the well-studied toxic effects of their ions is a critical but challenging measurement for nanotoxicity studies and regulation. This measurement is especially difficult for silver NPs (AgNPs) because in many relevant biological and environmental solutions, dissolved silver forms AgCl NPs or microparticles. Simulations predict that solid AgCl particles form at silver concentrations greater than 0.18 and 0.58 $\mu\text{g}/\text{mL}$ in cell culture media and moderately hard reconstituted water (MHRW), respectively. The AgCl NPs are usually not easily separable from AgNPs. Therefore, common existing total silver techniques applied to measure AgNP dissolution, such as inductively coupled plasma mass spectrometry (ICP-MS) or atomic absorption, cannot accurately measure the amount of silver remaining in AgNP form, as they cannot distinguish Ag oxidation states. In this work, we introduce a simple localized surface plasmon resonance (LSPR) UV–visible absorbance measurement as a technique to measure the amount of silver remaining in AgNP form for AgNPs with constant agglomeration states. Unlike other existing methods, this absorbance method can be used to measure the amount of silver remaining in AgNP form even in biological and environmental solutions containing chloride because AgCl NPs do not have an associated LSPR

absorbance. In addition, no separation step is required to measure the dissolution of the AgNPs. After using ICP-MS to show that the area under the absorbance curve is an accurate measure of silver in AgNP state for unagglomerating AgNPs in non-chloride-containing media, the absorbance is used to measure dissolution rates of AgNPs with different polymer coatings in biological and environmental solutions. We find that the dissolution rate decreases at high AgNP concentrations, 5 kDa polyethylene glycol thiol coatings increase the dissolution rate, and the rate is much higher in cell culture media than in MHRW.

Keywords Silver colloid · Dissolution · Silver ion · ICP-MS · Localized surface plasmon resonance absorbance

Introduction

Numerous studies have implicated the dissolution of metal ions from nanoparticles (NPs) in their toxicities because many metal ions used in NPs (e.g., Ag^+ , Zn^{2+} , Cu^{n+} , and Cd^{2+}) are well known to be toxic [1–12]. Researchers studying NP toxicity are concerned about NP-specific effects apart from the effects of their ions [4–6, 12–14]. Therefore, it is critical to develop methods to measure the dissolution of these NPs to distinguish between the toxicities of the metal NPs and the toxicities of their dissolved ions and ion complexes. Silver nanoparticles (AgNPs) in particular have been studied extensively due to their common and increasing use as anti-microbial agents and their demonstrated toxicity to certain cells and organisms [3–6, 8, 12]. However, it is still frequently unclear whether AgNP toxicity is caused by released silver ions, by the NPs themselves, or by a combination of NP and released ion effects (e.g., the “Trojan horse” effect [8, 13]).

Electronic supplementary material The online version of this article (doi:10.1007/s00216-011-5266-y) contains supplementary material, which is available to authorized users.

J. M. Zook (✉) · S. E. Long · D. Cleveland · C. L. A. Geronimo · R. I. MacCuspie
Material Measurement Laboratory,
National Institute of Standards and Technology,
100 Bureau Dr. MS 8313,
Gaithersburg, MD 20899, USA
e-mail: jzook@nist.gov

The most common methods used to measure dissolution of AgNPs are inductively coupled plasma-mass spectrometry (ICP-MS), inductively coupled plasma-optical emission spectrometry (ICP-OES), and atomic absorption (AA). All of these methods require that the silver ions be separated from the AgNPs before the measurements because they detect total silver content and not the silver oxidation state. This separation step has been done using centrifugation, ultrafiltration, and dialysis, each of which has potential artifacts. For example, centrifugation may not always sediment all of the smallest NPs unless very high centrifugal forces and long times are used (e.g., previous work showed that AgNPs smaller than 4 nm were not sedimented [15]). Ultrafiltration, which uses centrifugation or pressurized gas to force the solution through a nanoporous membrane, can separate even very small particles from the ions, but ions can adsorb to the membrane. This mass imbalance is especially significant for low concentrations of dissolved species. Dialysis takes a long time, often dilutes the sample, and can also lose ions due to membrane adsorption. Depending on the dissolution kinetics and the separation time, the AgNPs may dissolve significantly during the separation process for all methods. Finally, most environmental and biological solutions contain chloride ions, so that AgCl (and sometimes silver carbonate and silver phosphate) particles will form from the dissolved silver ions. At very high chloride concentrations, calculations based on equilibrium association constants predict that dissolved AgCl_2^- and AgCl_3^{2-} will form. However, many environmental and biological solutions contain only moderate concentrations of chloride. In these solutions, we calculate in the theory section that solid AgCl particles can constitute a large fraction of non-AgNP silver. Since AgCl particles cannot be distinguished from AgNPs with these ICP- and AA-based methods, they only measure the amount of silver in non-particulate form, and the total dissolution is underestimated. Other methods to measure ion dissolution include ion-selective electrodes and ion chromatography, which only measure Ag^+ ions and not strong silver complexes (e.g., with thiols, proteins, or chloride), again underestimating AgNP dissolution.

Because conventional methods used to measure AgNP dissolution cannot distinguish between AgNPs and AgCl NPs, they have typically only measured soluble dissolved forms of silver or have worked with low concentrations of AgNPs in which solid AgCl NPs do not form [3, 4, 6, 16–18]. Even complex measurement techniques such as laser postionization secondary neutral mass spectrometry/time-of-flight secondary ion mass spectrometry generally only measure silver concentrations and do not distinguish AgNPs from AgCl NPs [19]. In this work, we introduce a simple method using the UV–visible absorbance spectrum to measure AgNP dissolution in various solutions contain-

ing moderate (5 $\mu\text{g/mL}$) to high (100 $\mu\text{g/mL}$) AgNP concentrations. AgNPs are well known to have a localized surface plasmon resonance (LSPR) peak, which causes a peak absorbance near 400 nm for unagglomerated particles and shifts to longer wavelengths for agglomerated particles. The peak absorbance has previously been used as an estimate of AgNPs remaining as single NPs when agglomeration is occurring, since the absorbance at the peak decreases when AgNPs agglomerate and sediment [16, 20–22]. However, for unagglomerating NPs, decreases in absorbance can be used as a measure of dissolution. Because AgCl particles do not have an LSPR peak, it is expected that this absorbance-based method is one of the only methods that can measure AgNP dissolution rates in situ from moderate to high AgNP concentrations in many solutions containing chloride ions.

Materials and methods

Certain commercial equipment, instruments, or materials are identified in this report to specify adequately the experimental procedure. Such identification does not imply recommendation or endorsement by the National Institute of Standards and Technology (NIST), nor does it imply that the materials or equipment identified are necessarily the best available for the purpose. Unless stated otherwise, all chemicals were ACS reagent grade and used as received without further purification.

Synthesis of AgNPs

Citrate-stabilized AgNPs (~23 nm intensity-weighted mean diameter in water by DLS) were produced using a previously described method of reducing an aqueous solution of boiling silver nitrate in the presence of trisodium citrate dihydrate with sodium borohydride obtained from Sigma Aldrich (St. Louis, MO, USA) [20]. The AgNPs were coated with different polymers by ligand exchange. The polymer coatings used were two different sizes of poly(ethylene glycol)-thiols (5 kDa PEG and 20 kDa PEG) from Nanocs (New York, NY, USA, #PEG3-0021 and #PEG3-0025, respectively), and approximately 10 kDa poly(vinyl pyrrolidone) (PVP) and dextran from Sigma-Aldrich (#PVP10 and #D9260, respectively). Specifically, ~60 $\mu\text{g/mL}$ citrate-coated AgNPs were mixed with 1 mmol/L of each polymer at a 9:1 volume ratio. The reaction was allowed to proceed for 1 h. Each of the samples was concentrated to 1 mg/mL by nitrogen-pressurized ultrafiltration (Millipore 8200) using a regenerated cellulose 100-kDa relative molecular weight cutoff membrane so that free ligands were mostly (>90%) separated from the AgNPs. Characterization of purified stocks of functionalized AgNPs can

be found in Electronic Supplementary Material Figs. S1, S2, S3, S4, S5, and S6.

For the experiments comparing absorbance and ICP-MS, both PEG-AgNPs were dispersed in 0.1 mol/L HNO₃ at 5 µg/mL. Because they dissolve quickly in HNO₃, the absorbance of the NPs at 5 µg/mL in deionized water was used as the baseline absorbance. The citrate-AgNPs were dispersed in 0.15 mol/L KNO₃+2% bovine serum albumin (BSA) with two different recently described methods [23], depending on the desired agglomeration state. To obtain well-dispersed AgNPs, the AgNPs were pipetted directly into KNO₃/BSA while vortexing at maximum speed. To obtain agglomerates, AgNPs were first dispersed at 200 µg/mL in 0.15 mol/L KNO₃ and allowed to agglomerate to the desired mean size before diluting 1:1 with 0.15 mol/L KNO₃+4% BSA. The samples were then immediately diluted to 5 µg/mL AgNPs with deionized water, since the agglomerates were more stable in this diluted solution.

After measuring the absorbance at the desired time point as described below, the samples were immediately centrifuged at 20,800×*g* for 30 min at 2 °C to pellet the undissolved AgNPs. Finally, the supernatant was taken and diluted with 0.1 mol/L HNO₃ for measurement by ICP-MS. In addition, the AgNPs were diluted directly into 0.1 mol/L HNO₃ without centrifugation in order to measure the total silver concentration with ICP-MS. Also, since the AgNPs were used 2 to 5 months after they were prepared, some silver may have dissolved prior to the experiments. Therefore, the AgNPs were centrifuged in deionized water, and the supernatant was then measured with ICP-MS in order to measure the initial concentration of silver ions and/or AgNPs too small to sediment. The initial non-sedimented weight fractions were about 4.5% for citrate-AgNPs, and 24% and 22% for 5- and 20-kDa PEG-AgNPs, respectively. The higher initial “dissolved” fraction for PEG-AgNPs may be due to the longer time between their preparation and use (5 months for PEG vs. 2 to 3 months for citrate) or due to the slower sedimentation of PEG-AgNPs. This initial dissolved silver concentration was subtracted from all other measurements when calculating the dissolution rate.

Dynamic light scattering (DLS)

For characterization of functionalized AgNP stocks, the DLS methodology followed recommendations outlined in the NIST-Nanotechnology Characterization Laboratory Assay Cascade Protocol PCC-1 [24]. DLS measurements were performed using a Malvern Instruments (Westborough, MA, USA) Zetasizer Nano in 173° backscatter mode or Brookhaven Instruments (Brookhaven, NY, USA) Zeta-PALS at a 90° angle at 20.0 °C. Sample preparation was performed in a particle-free hood. Disposable semi-micro cuvettes were cleaned and dried immediately before use.

The cumulants analysis algorithm was applied to obtain the Z_{avg} equivalent hydrodynamic diameter. Samples were vortexed immediately prior to measurement in order to avoid artifacts from sedimentation of agglomerates. Diameter values reported are the mean of five consecutive measurements, with one standard deviation representing the precision of the observed mean.

ICP-MS

Samples were stored in the dark in a refrigerator at 4 °C prior to analysis. Analyses were completed within 3 days of sample preparation. Prior to analysis, the samples were removed from the refrigerator and allowed to reach normal laboratory temperature (20 °C to 25 °C). An aliquot of indium internal standard was added to each tube, and the samples were then diluted to 14.75 mL using high-purity de-ionized water.

Determinations of silver were made using a Thermo X7 ICP-MS instrument (Thermo Electron, Winsford, Cheshire, UK) operating in conventional (not collision cell technology) pulse counting mode. Five blocks of data, each 30 s in duration, were acquired for each sample at mass/charge (*m/z*) 109 (Ag) and 115 (In) using peak jumping and a dwell time of 10 ms. Quantitative measurements were made using external calibration. The calibration standard, having a concentration of 9.77 ng/mL, was prepared in the laboratory by serial dilution of a high-purity primary standard (NIST SRM 3151, Silver Standard Solution, lot number 992212). The sample run sequence was randomized with the calibration standard measured at the beginning, middle, and end of the measurement run. Silver measurements by ICP-MS can be problematic owing to memory effects from silver adsorption on material surfaces resulting in sample-to-sample cross-talk. However, in this case, the instrument background was found to return to normal and stabilize within 2 min of washout with the instrument rinse solution (2% mass fraction nitric acid), and no specialized wash solutions were required. The expanded uncertainties of the ICP-MS measurements (calculated from the combined uncertainties of replicate measurements, calibration measurements, primary calibrant, instrument mass discrimination drift, instrument dead-time correction effects, instrument background correction, and weighing measurements [25]) were approximately 2% of the measured mean values.

Absorbance measurements

Spectrophotometric absorbance measurements between 300 and 1,100 nm were made using a Hewlett Packard 8453 spectrophotometer (Palo Alto, CA, USA). Samples were vortexed immediately prior to measurement in order to avoid artifacts from sedimentation of agglomerates. The absorbance of the 5-µg/mL AgNPs was measured directly in a 1-cm

quartz cuvette. The 100- $\mu\text{g}/\text{mL}$ AgNPs were diluted 20 \times with water immediately before each absorbance measurement. The appropriate background absorbance of Dulbecco's modified Eagle's medium (DMEM)+2% BSA was subtracted from the spectra of AgNPs dispersed in DMEM. To minimize effects of slight changes in the baseline, the baseline (calculated as the mean absorbance between 900 and 1,100 nm) was subtracted from every curve. In addition, scattering due to AgCl NPs was approximated by assuming Rayleigh scattering (so absorbance is proportional to λ^{-4}) and setting the absorbance at 325 nm (Abs_{325}) to 5.5% of the peak absorbance Abs_{400} , resulting in the equation $\text{Abs}_{\text{AgCl}} = (\text{Abs}_{325} - 0.055 \times \text{Abs}_{400}) \times (\lambda/325)^{-4}$. The absorbance at 325 nm was chosen for fitting because unagglomerated AgNPs have a minimum at 325 nm, and 5.5% was used because Abs_{325} is 5.5% of Abs_{400} for unagglomerated AgNPs. This factor was subtracted from every spectrum. This correction factor will be most accurate when AgCl NPs are small, since deviations from Rayleigh scattering become significant when the NPs are not much smaller than the wavelength of light.

The absorbance curve was integrated from 340 to 650 nm for the integrated absorbance, or the peak absorbance (~ 395 nm) was found. Despite the complexity of reactions occurring (e.g., silver ions complexing with other species), dissolution rates were found to approximately fit first order kinetics (i.e., $\text{Abs} = \text{Abs}_0 e^{-kt}$). The first order rate constant k was found by plotting $\ln(\text{absorbance})$ vs. time for the first 22 h and fitting a straight line.

Dissolution in biological and environmental media

DMEM, pH 7.4, with 4.5 g/L glucose and sodium pyruvate but without phenol red or L-glutamine was obtained from Mediatech (Manassas, VA, USA). Bovine serum albumin (BSA) was from Sigma Aldrich (St. Louis, MO, USA; $\geq 96\%$, essentially fatty acid free). The antibiotics streptomycin and penicillin were from Invitrogen and were added at 100 $\mu\text{g}/\text{mL}$ and 100 U/mL, respectively, to DMEM to reduce bacterial growth. DMEM+4% BSA and 0.15 mol/L KNO_3 +4% BSA by weight were filtered through a 0.2- μm polypropylene syringe filter to remove large protein aggregates that would interfere with the DLS measurements. Preparation of EPA moderately hard reconstituted water (MHRW) followed the procedure described elsewhere [26]. A stock solution of humic acid was prepared by dissolving Suwannee River Humic Acid Standard II (#2S101H, International Humic Substances Society, St. Paul, MN, USA) in deionized water at 1 mg/mL, then diluted into MHRW at the desired working concentration.

The absorbance spectra of citrate-, dextran-, PVP-, and both PEG-stabilized AgNPs were monitored over time in DMEM+2% BSA and in MHRW+10 $\mu\text{g}/\text{mL}$ humic acids.

The AgNPs were dispersed at 5 or 100 $\mu\text{g}/\text{mL}$ to determine the effect of AgNP concentration on dissolution. To obtain well-dispersed NPs, they were dispersed in both solutions by pipetting a 50- or 1,000- $\mu\text{g}/\text{mL}$ AgNP solution into the media while vortexing at maximum speed. The initial absorbance measurement was made within 1 min of dispersing the AgNPs. The solutions were stored at room temperature and measured 1, 2, 3.5, 5, 22, and 46 h after dispersion.

All statistical comparisons were performed in Matlab (Natick, MA, USA) using the one-way ANOVA test with Tukey's honestly statistically different test to compare the individual means.

Simulations of equilibrium proportions of aqueous silver and AgCl particles

Simulations were performed to determine how silver from AgNO_3 (a model for silver dissolved from AgNPs) partitions between all aqueous silver forms (which remain in solution after centrifugation) and AgCl particles (which are in the pellet after centrifugation) in solutions containing various relevant concentrations of chloride. Simulations were performed with the freely available program GeoChem-EZ [27] to calculate how much silver is in aqueous and in $\text{AgCl}(\text{s})$ particulate forms at equilibrium. We specified only the concentrations of silver and chloride, keeping all parameters as their default values except allowing solids to precipitate.

Theory

Effect of chloride ions on AgNP dissolution measurement techniques

Here, we simulate how silver that has dissolved from AgNPs (modeled as AgNO_3 in a solution) speciates between aqueous and AgCl particulate forms in order to predict when ICP-MS and AA will not measure the total amount of silver that has dissolved from AgNPs. As described in the "Introduction" section, chloride ions will often form AgCl particles from silver that dissolves from AgNPs. Therefore, chloride can have a significant effect on all AgNP dissolution measurement techniques that rely on separating dissolved silver from particulate silver using centrifugation and/or filtration membranes (e.g., ICP-MS and AA) or that only measure dissociated Ag^+ ions (e.g., ion-selective electrodes). The impact of chloride on these measurement techniques depends on both the silver concentration and the chloride concentration, since silver can be in several aqueous forms (Ag^+ , $\text{AgCl}(\text{aq})$, AgCl_2^- , AgCl_3^{2-} , and AgCl_4^{3-}), as well as in particulate form (AgNP and $\text{AgCl}(\text{s})$). We calculated the proportion of silver in all aqueous forms because these forms

are measured by ICP-MS and AA after centrifugation, whereas AgCl(s) particles are sedimented into the pellet with any AgNPs and are not measured. The dissolution kinetics of silver released from AgNPs is generally slower than the kinetics of formation of forms of silver that arise from the silver ions. Thus, a calculation was performed to estimate the dissolved fraction of silver that would exist for various concentrations of AgNO₃ added to a chloride-containing solution, as a model of equivalent concentrations of silver dissolved from AgNPs. Predictions of the fraction of silver that would exist in aqueous form (i.e., measured by ICP-MS or AA) were determined for chloride concentrations of 0.01, 0.054 (MHRW), 119 (DMEM), and 339 mmol/L (seawater [28]).

As shown in Table 1, these simulations predict that at equilibrium, silver from AgNO₃ (or dissolved AgNPs) is entirely in aqueous form at very low silver concentrations. At higher silver concentrations of 5 and 100 µg/mL, the highest concentration of AgCl particles occurs around physiological chloride concentrations. It should be noted that increasing concentrations of silver do not necessarily create higher concentrations of aqueous silver species, since AgCl has a limited solubility (e.g., at physiological chloride concentrations, the total aqueous silver is 0.18 µg/mL for total silver concentrations of 5 or 100 µg/mL). Therefore, for silver concentrations higher than those in the first four rows of Table 1, typical methods of measuring AgNP dissolution that cannot distinguish AgCl NPs from AgNPs (e.g., ICP-MS or AA) could show that dissolved silver has reached an “equilibrium” state when in fact silver is still dissolving from AgNPs and forming AgCl particles.

These calculations do not include non-chloride AgNP- and Ag⁺-complexing agents (such as L-cysteine, which is at a concentration of 0.32 mmol/L in typical DMEM formulations), which will likely cause higher soluble silver fractions than in these calculations. However, since UV–visible absorbance measurements show light scattering from non-

AgNP particles after dissolution of 5 µg/mL AgNPs, it appears likely that AgCl particles form even when the total concentration of silver is much smaller than cysteine. We measure AgCl particles even in the presence of cysteine probably because the concentration of chloride is very high, and the AgCl association constant is very large. This result is consistent with recent simulations, which predicted that solid AgCl will predominate at extracellular thiol concentrations for 1 mmol/L total silver [17].

AgNPs and Beer's law

Beer's law for a solution containing dissolving AgNPs can be written as:

$$A = \sum \epsilon_i b c_i \tag{1}$$

where ϵ_i is the absorptivity of species i , b is the path length, and c_i is the concentration of species; species 1 is unagglomerated AgNPs, species 2 is various AgNP agglomerates, species 3 is silver ions or very small AgNPs, and species 4 is the extinction due to scattering from AgCl particles. Typically, ϵ_3 is close to zero. If the AgNPs are the only light-absorbing species in the solution and are singly dispersed, so that $c_2=0$, or the absorbance of non-AgNP components is constant or can be subtracted (e.g., AgCl particles), then the absorbance after 100% dissolution should be zero. Beer's law then dictates the mass of the remaining AgNPs is directly proportional to the absorbance. However, because AgNPs are expected to decrease in size during dissolution, the observed absorbance may not hold Beer's law linearity if the absorptivity of AgNPs changes significantly with size (i.e., if ϵ_1 changes). Additionally, different sizes of agglomerates exhibit different absorbance spectrum changes (i.e., ϵ_2 changes) [23], and larger agglomerates can sediment out of solution (i.e.,

Table 1 Calculated equilibrium quantity of aqueous silver (vs. solid AgCl) with chloride at various relevant environmental and biological concentrations (not including other Ag⁺-complexing agents) from AgNO₃ or silver dissolved from AgNPs

Media ([Cl ⁻] in mmol/L)	[Ag] in µg/mL (mmol/L) dissolved from AgNPs	Percent aqueous Ag (µg/mL)
Low Cl ⁻ (0.01)	<2.4 (0.022) ^a	100 (2.4)
MHRW ^b (0.054)	<0.48 (0.0044) ^a	100 (0.48)
DMEM ^c (119)	<0.18 (0.0017) ^a	100 (0.18)
Seawater (339)	<1.0 (0.0093) ^a	100 (1.0)
Low Cl ⁻ (0.01)	5 (0.046)	90.8 (4.54)
MHRW ^b (0.054)	5 (0.046)	26.4 (1.32)
DMEM ^c (119)	5 (0.046)	3.60 (0.18)
Seawater (339)	5 (0.046)	20.8 (1.04)
Low Cl ⁻ (0.01)	100 (0.93)	98.1 (98.1)
MHRW ^b (0.054)	100 (0.93)	94.4 (94.4)
DMEM ^c (119)	100 (0.93)	0.18 (0.18)
Seawater (339)	100 (0.93)	1.03 (1.03)

^a Maximum concentrations of silver for which 100% is in aqueous form (i.e., no AgCl particles)

^b MHRW based on chloride in moderately hard reconstituted water

^c DMEM based on chloride in cell culture media

c_2 changes). Also, NPs may adsorb to surfaces of the container, although these effects were considered to be negligible in these experiments. The smallest AgNPs (<4 nm) stay in the supernatant and are thus measured by ICP-MS as “dissolved”, but ε_3 and their LSPR is nearly zero, so they are also measured as “dissolved” by the absorbance method. These last two competing effects may appear to cancel to some extent, keeping close agreement to the 1:1 correlation line between techniques in Fig. 1. However, most of these possibilities would cause the absorbance to decrease more than expected (causing points above the 1:1 correlation line in Fig. 1), but shifts in absorbance due to agglomeration can cause the area under the absorbance curve to increase (causing points below the 1:1 correlation line in Fig. 1). Therefore, to determine under which conditions Beer's law can be used to quantify AgNP dissolution, with tolerable deviations from the 1:1 correlation, we have compared the absorbance changes to the dissolved Ag measured by centrifugal separation and ICP-MS.

Results and discussion

Method validation with ICP-MS in solutions without chloride

To determine the conditions under which the absorbance-based method is appropriate to measure AgNP dissolution, we compared either the decrease in peak absorbance or the

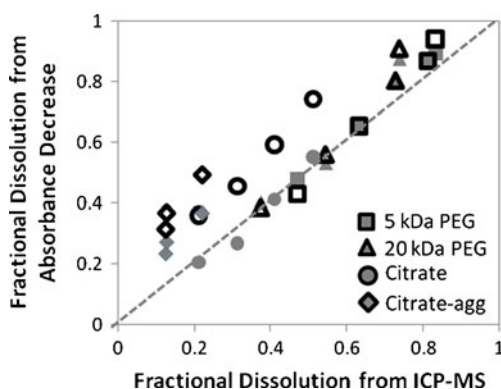


Fig. 1 Comparison of fractional dissolution of AgNPs measured by decrease in absorbance to dissolution measured by ICP-MS. The decrease in absorbance was calculated from the peak at ~ 400 nm (empty black symbols) or from the integrated area under the absorbance curve (filled grey symbols). Dissolution was measured for AgNPs coated with (1) 5 kDa PEG-thiol (squares) and (2) 20 kDa PEG-thiol (triangles) in 100 mmol/L HNO_3 , (3) citrate-coated AgNPs dispersed as primary particles in 150 mmol/L KNO_3 +2% BSA (circles), and (4) citrate-coated AgNPs dispersed as agglomerates that grow over 5 days from 230 to 780 nm (DLS intensity-weighted mean diameters) in 7.5 mmol/L KNO_3 +0.1% BSA (diamonds). The diagonal dotted grey line indicates the 1:1 correlation expected from Beer's law. Standard deviations for replicated absorbance and ICP-MS measurements of the same sample are smaller than the symbols

integrated area under the absorbance spectrum to the dissolved silver measured by ICP-MS after centrifuging down the AgNPs. To validate the absorbance-based method with ICP-MS, we tested four different solutions that cause AgNPs to dissolve rapidly but do not contain chloride. Specifically, absorbance and ICP-MS were compared for (1) AgNPs coated with 5 kDa PEG-thiol in 100 mmol/L HNO_3 , (2) AgNPs coated with 20 kDa PEG-thiol in 100 mmol/L HNO_3 , (3) citrate-coated AgNPs dispersed as primary particles in 150 mmol/L KNO_3 +2% BSA, and (4) citrate-coated AgNPs dispersed as agglomerates that grow over 5 days from 230 to 780 nm (DLS intensity-weighted mean diameters) in 7.5 mmol/L KNO_3 +0.1% BSA.

The PEG-coated AgNPs were chosen for method validation because they are stable against agglomeration in most high ionic strength solutions. DLS was used to characterize the polymer coatings on the AgNPs, which has been successfully used previously to measure the increase in size after polymer coating [29, 30]. We found that the mean intensity-weighted diameters and standard deviations were 21.1 ± 0.1 , 40.6 ± 0.6 , 62.8 ± 0.8 , 25.0 ± 0.2 , and 22.1 ± 0.3 nm for AgNPs coated with citrate, 5-kDa PEG, 20-kDa PEG, PVP, and dextran, respectively. All polymer-coated AgNPs were statistically significantly larger than the citrate-coated AgNPs ($p < 0.05$). Both types of PEG-coated AgNPs dissolve by about 80% within 4 h in 100 mmol/L HNO_3 (see Electronic Supplementary Material Fig. S7 for plots showing dissolution vs. time), showing an approximately 1:1 correlation between dissolution and the decrease in either peak absorbance or area under the absorbance curve (5 and 20 kDa PEG are represented by squares and triangles, respectively, in Fig. 1). In Fig. 1, the proportional dissolution measured by the absorbance decrease is compared to the dissolution measured by ICP-MS, with the diagonal dotted line indicating a 1:1 correlation between absorbance decrease and dissolution. Figure 2a shows an example of the absorbance decrease over time for 5 kDa PEG-coated AgNPs, used to construct Fig. 1. The final time point at 21 h shows slightly more decrease in absorbance than expected, which may be a result of slight agglomeration of the remaining AgNPs after long times in the acidic solution.

The citrate-coated AgNPs dispersed as single NPs (i.e., no LSPR absorbance shift) were also stable against agglomeration as a result of the high BSA concentration coating the NPs. These AgNPs dissolved by about 50% in 27 h in 0.15 mol/L KNO_3 +2% BSA (Electronic Supplementary Material Fig. S7), showing an approximately 1:1 correlation between dissolution and the decrease in area under the absorbance curve (filled circles in Fig. 1). However, the peak absorbance decreases more than expected, indicating that the area under the absorbance curve is more robust towards slight shifts in the LSPR

absorbance spectrum, which could be caused by changes in the dielectric constant around the AgNPs or association between AgNPs.

Finally, as a more complex system, we tested citrate-coated AgNPs dispersed as agglomerates. Unlike in cell culture media [23] we were unable to find conditions in KNO_3 in which the agglomerates remained constant in size. In this situation, there is not a 1:1 correlation between dissolution and absorbance, even when measuring the area under the absorbance curve (see diamonds in Fig. 1). Instead, the absorbance decreases more than expected, which is probably due to changes in the NP agglomeration state that cause the LSPR absorbance spectrum to change. Even though the net absorbance spectrum decreases fairly uniformly across all wavelengths, as shown in Fig. 2b, the size measured by DLS increases significantly from 231 to 521 nm over 25 h, indicating that some additional agglomerates are formed over time despite the presence of

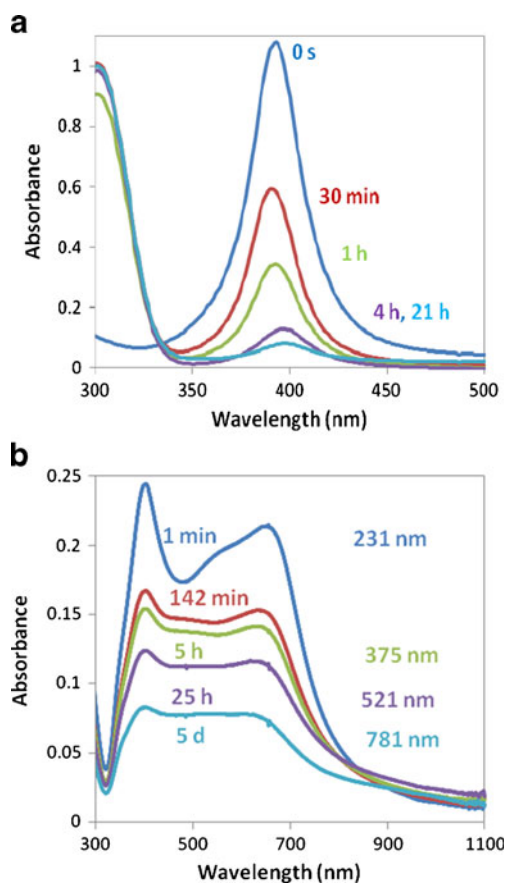


Fig. 2 Absorbance spectra at several time points illustrating how the absorbance decreases as the AgNPs dissolve for (a) 5 kDa PEG-coated AgNPs that remain stable in size (as measured by DLS) over 21 h in 0.1 mol/L HNO_3 (squares in Fig. 1). (b) Citrate-coated AgNPs dispersed as agglomerates that grow in size over 5 days from 231 to 781 nm (DLS intensity-weighted mean diameters, as labeled on the right side of the figure) in 7.5 mmol/L KNO_3 +0.1% BSA (diamonds in Fig. 1). Spectra for other dissolution experiments are shown in Electronic Supplementary Material Fig. S8

excess BSA. Similar results are obtained for slightly larger agglomerates depicted in Electronic Supplementary Material Fig. S8. Therefore, absorbance may not provide an accurate estimate of dissolution in systems in which the agglomeration state changes over time. However, by monitoring the particle size by DLS, one can ensure the validity of the absorbance method for the system of interest.

To assess statistical agreement between the ICP-MS and absorbance-based methods, we used a method published previously [31], in which the mean and twice the standard deviation (SD) of the difference between the two methods gives the bias and “limits of agreement” (i.e., the deviation from the 1:1 correlation line in Fig. 1). When subtracting the ICP-MS measurement from the area under the absorbance curve for the 5-kDa PEG, 20-kDa PEG, and

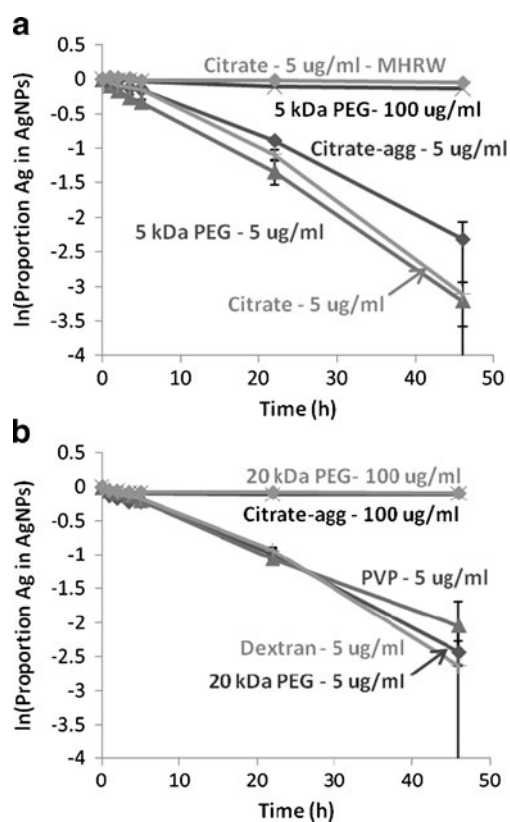


Fig. 3 Proportional AgNP dissolution over 46 h as measured by area under the absorbance curve for AgNPs at 5 and 100 $\mu\text{g/mL}$ with 5 kDa PEG-thiol, 20 kDa PEG-thiol, citrate, PVP, and dextran coatings (as labeled in (a) and (b)) in DMEM+2% BSA (except for one experiment in MHRW labeled “Citrate-5 $\mu\text{g/mL}$ -MHRW”). (a) and (b) are separated to minimize overlapping curves but are identical conditions otherwise. The curves labeled “Citrate-agg” are slightly agglomerated since they were prepared at 100 $\mu\text{g/mL}$ and agglomerated slightly before they could be coated with BSA. Points represent the mean of three different samples. Error bars represent standard deviations, which are calculated from three separately prepared samples before taking the natural logarithm. Error bars not shown are smaller than the symbols. First-order kinetics predict a linear curve when plotting $\ln(\text{proportion Ag in AgNP form})$ vs. time. Lines are shown to guide the eye

unagglomerated citrate-coated AgNPs with dissolution between 20% and 70%, we get a bias $\pm 2 \times \text{SD}$ of $-0.5\% \pm 5.4\%$. Therefore, we would expect most absorbance measurements of dissolution will be less than 5.9% different from the ICP-MS measurement in solutions without chloride.

AgNP dissolution rates in biological and environmental media

To demonstrate the utility of this absorbance-based method in biological and environmental samples, we have compared dissolution rates of AgNPs (1) with different polymer coatings, (2) at different total silver concentrations, (3) in different solutions (i.e., DMEM-BSA or MHRW-humic acid), and (4) in different agglomeration states. We recently developed a method to produce relatively stable agglomerates of various types of NPs, including AgNPs, in the cell culture media DMEM by stabilizing them with 2% BSA [23]. We can also produce relatively stable AgNPs in a synthetic environmental solution (MHRW) by stabilizing with humic acids. When the agglomeration state does not change significantly over time, the absorbance spectrum decreases uniformly over all wavelengths, and the integrated absorbance is expected to be a good measure of dissolution. Extinction due to Rayleigh and Mie light scattering from AgCl particles only starts to become significant when most of the AgNPs have dissolved, and Rayleigh scattering can be subtracted as described in “Materials and methods” section.

Based on the ICP-MS results in Fig. 1, the area under the absorbance curve gives the best estimate of dissolution. However, the area under the absorbance curve may slightly underestimate dissolution since this area often increases as agglomeration increases, and we found the spectra to often broaden slightly over time indicating small amounts of agglomeration (see Electronic Supplementary Material Fig. S9). Therefore, the peak absorbance can probably be used as an upper bound on the dissolution rate, and the area under the absorbance curve gives a better estimate and can often be used as a lower bound.

We tested the effect of a variety of common polymer coatings on dissolution of the AgNPs because we hypothesized that they may affect dissolution rate either by slowing the diffusion coefficient through the polymer or by preventing BSA from coating the AgNPs. Although DLS could not measure decreases in NP size over time due to the large scattering signal from BSA, DLS is much more sensitive to increases in NP size resulting from agglomeration. DLS did not show an increase in size over time for any of the samples, so agglomeration was not expected to significantly interfere with the absorbance-based method (i.e., $c_2 \approx 0$ in Eq. 1).

Figure 3 shows the fractional dissolution over time for each experiment, and Table 2 contains the first order dissolution rate constants (k) during the initial 22 h for each dispersion of AgNPs. The rates were calculated from both the area under the absorbance curve and the peak absorbance. In DMEM, the dissolution rates based on area were between 3.8%/h and 5.5%/h for all the polymer

Table 2 Dissolution rates over 22 h of 5 and 100 $\mu\text{g}/\text{mL}$ AgNPs with different polymer coatings in cell culture media (DMEM) and moderately hard reconstituted water (MHRW)

Polymer coating	Solution	[AgNP] ($\mu\text{g}/\text{mL}$)	Dissolution rate (k) from area ^d (%/h)	Dissolution rate (k) from peak ^d (%/h)
Citrate-agg ^a	DMEM	5	4.0 \pm 0.1	5.6 \pm 0.3
5 kDa PEG	DMEM	5	6.0 \pm 0.8	10.3 \pm 0.8
20 kDa PEG	DMEM	5	4.3 \pm 0.4	8.1 \pm 0.5
Citrate ^b	DMEM	5	5.0 \pm 0.4	7.7 \pm 0.2
Dextran	DMEM	5	4.2 \pm 0.2	7.1 \pm 0.2
PVP	DMEM	5	4.9 \pm 0.2	8.1 \pm 0.1
Citrate ^c	MHRW	5	0.2 \pm 0.2	0.9 \pm 0.3
Citrate-agg ^a	DMEM	100	0.3 \pm 0.1	0.4 \pm 0.1
5 kDa PEG	DMEM	100	0.4 \pm 0.1	0.7 \pm 0.1
20 kDa PEG	DMEM	100	0.2 \pm 0.2	0.7 \pm 0.2

^a Citrate-agg AgNPs were dispersed at 100 $\mu\text{g}/\text{mL}$ to create controlled/stable agglomerates prior to BSA coating, then were diluted to working concentrations

^b Citrate AgNPs that were singly dispersed likely adsorbed a significant BSA coating from the DMEM media

^c Citrate AgNPs that were singly dispersed likely adsorbed a significant humic acid coating from the MHRW media

^d Dissolution rates (k) were calculated in order to compare dissolution at different concentrations. The rates were calculated for each of the three replicated samples from either the area under the absorbance curve (expected to be the best estimate and the lower bound) or the peak absorbance (expected to be the upper bound) over the first 22 h and reported as mean \pm one standard deviation ($n=3$)

coatings at 5 $\mu\text{g}/\text{mL}$. The rates were significantly higher for the 5-kDa PEG-thiol-coated AgNPs than for any of the others ($p < 0.05$, except citrate-coated for which $p < 0.06$). The rates may be higher for these NPs because the 5-kDa PEG prevents BSA from coating the particles and is a relatively low molecular weight coating.

The dissolution rates are much higher for 5 $\mu\text{g}/\text{mL}$ AgNPs than for 100 $\mu\text{g}/\text{mL}$ (all are significantly different with $p < 0.01$). This difference may result from the higher ratio of dissolved silver ions to silver complexing agents (which may act as a dissolution product scavenger) or from silver ions associating back with the AgNPs at high concentrations. Dissolution is insignificant from 5 to 46 h for 100 $\mu\text{g}/\text{mL}$ 20-kDa PEG- and citrate-AgNPs (see Fig. 3b). Light scattering by AgCl NPs is insignificant for moderate dissolution, but it starts to contribute significantly to the absorbance for the 5- $\mu\text{g}/\text{mL}$ AgNP samples at the 22- and 46-h time points when most of the AgNPs have dissolved. This scattering is subtracted from the spectra by modeling the scattering as dependent on λ^{-4} (as described in “Materials and methods” section). Although the 46-h time points are included in Fig. 3 for completeness, the systematic biases and random errors associated with them are quite large because the extinction due to scattering is larger than LSPR absorbance. Therefore, the 46-h time points are not included in the dissolution rate calculations.

The dissolution rates were much higher ($p < 0.01$) in DMEM-BSA than in MHRW-humic acid, possibly due to the much higher chloride concentration in DMEM. Higher chloride concentration may cause faster dissolution because chloride forms complexes with silver ions.

The small amount of agglomeration in the citrate-coated AgNPs dispersed at 100 $\mu\text{g}/\text{mL}$ and then diluted to 5 $\mu\text{g}/\text{mL}$ (“Citrate-agg” in Table 2) results in less dissolution than the same NPs well-dispersed at 5 $\mu\text{g}/\text{mL}$ ($p < 0.05$). Agglomeration may decrease the dissolution rate because agglomerates have a lower specific surface area from which silver ions can dissolve.

Conclusions

In contrast to other methods used to measure AgNP dissolution, this absorbance-based method is expected to be able to measure the dissolution rate in biologically and environmentally relevant chloride-containing solutions because only AgNPs (not AgCl particles) have an absorbance associated with LSPR. When the majority of AgNPs have dissolved, interference from extinction due to light scattering from AgCl particles is subtracted from the total absorbance by modeling it as a wavelength-dependent absorbance. However, this method is still subject to interference from changing agglomeration states, so other

methods should be used to confirm agglomeration is not occurring. Fortunately, AgNPs are stable against agglomeration in many realistic biological and environment media, including the cases used in this work, in which the AgNPs were stabilized either by polymer coatings or by common proteins or natural organic matter. Decreases in area under the UV-visible absorbance curve are approximately equivalent to dissolution of AgNPs for moderate to high concentrations of well-dispersed AgNPs measured by ICP-MS in solutions without chloride (e.g., in nitric acid and in KNO_3 with BSA). The dissolution rates of AgNPs with different polymer coatings were compared in complex biological and environmental media. Five-kDa PEG coatings significantly increase the dissolution rate, and greater molecular weight coatings significantly decrease the dissolution rate. The lower detection limit is expected to be limited by the absorptivity of AgNPs, likely limited to changes of about 50 ng/mL , which corresponds to an absorbance change of ~ 0.01 for a 1-cm path length. This detection limit is sufficient for many AgNP cytotoxicity studies [23]. While this detection limit is higher than the lowest concentrations found in the environment, where the quantitative dissolution rates may be different, the qualitative comparison of dissolution rates between different types of AgNPs at moderate concentrations can probably be extrapolated to lower concentrations. Other dissolution measurement methods begin to be inaccurate when AgCl particles start to form (e.g., at silver concentrations above 0.48 $\mu\text{g}/\text{mL}$ in MHRW and above 0.18 $\mu\text{g}/\text{mL}$ in DMEM). Above these concentrations, we expect that our absorbance-based measurement method will especially be useful for nanotoxicity studies in environmental and biological solutions containing chloride because it is frequently desired to distinguish toxic effects of AgNPs (which are generally not well-understood) from the effects of silver ions (which may form various silver complexes such as AgCl, but have been studied much more). Specifically, it will help determine whether AgNPs should be treated differently from other forms of silver from a regulatory perspective.

References

1. Prabhu BM, Ali SF, Murdock RC, Hussain SM, Srivatsan M (2010) Copper nanoparticles exert size and concentration dependent toxicity on somatosensory neurons of rat. *Nanotoxicology* 4:150–160
2. Unrine JM, Tsyusko OV, Hunyadi SE, Judy JD, Bertsch PM (2010) Effects of particle size on chemical speciation and bioavailability of copper to earthworms (*Eisenia fetida*) exposed to copper nanoparticles. *J Environ Qual* 39:1942–1953
3. Sotiriou GA, Pratsinis SE (2010) Antibacterial activity of nano-silver ions and particles. *Environ Sci Technol* 44:5649–5654
4. Yeo MK, Yoon JW (2009) Comparison of the effects of nano-silver antibacterial coatings and silver ions on zebrafish embryogenesis. *Mol Cell Toxicol* 5:23–31

5. Miura N, Shinohara Y (2009) Cytotoxic effect and apoptosis induction by silver nanoparticles in HeLa cells. *Biochem Biophys Res Commun* 390:733–737
6. Liu JY, Hurt RH (2010) Ion release kinetics and particle persistence in aqueous nano-silver colloids. *Environ Sci Technol* 44:2169–2175
7. Sopjani M, Foller M, Haendeler J, Gotz F, Lang F (2009) Silver ion-induced suicidal erythrocyte death. *J Appl Toxicol* 29:531–536
8. Park EJ, Yi J, Kim Y, Choi K, Park K (2010) Silver nanoparticles induce cytotoxicity by a Trojan-horse type mechanism. *Toxicol Vitr* 24:872–878
9. Lee J, Ji K, Kim J, Park C, Lim KH, Yoon TH, Choi K (2010) Acute toxicity of two CdSe/ZnSe quantum dots with different surface coating in *Daphnia magna* under various light conditions. *Environ Toxicol* 25:593–600
10. Poynton HC, Lazorchak JM, Impellitteri CA, Smith ME, Rogers K, Patra M, Hammer KA, Allen HJ, Vulpe CD (2010) Differential gene expression in *Daphnia magna* suggests distinct modes of action and bioavailability for ZnO nanoparticles and Zn ions. *Environ Sci Technol* 45:762–768
11. Zhang LW, Monteiro-Riviere NA (2009) Mechanisms of quantum dot nanoparticle cellular uptake. *Toxicol Sci* 110:138–155
12. Lubick N (2008) Nanosilver toxicity: ions, nanoparticles or both? *Environ Sci Technol* 42:8617
13. Limbach LK, Grass RN, Stark WJ (2009) Physico-chemical differences between particle- and molecule-derived toxicity: can we make inherently safe nanoparticles? *Chimia* 63:38–43
14. Hussain SM, Braydich-Stolle LK, Schrand AM, Murdock RC, Yu KO, Mattie DM, Schlager JJ, Terrones M (2009) Toxicity evaluation for safe use of nanomaterials: recent achievements and technical challenges. *Adv Mater* 21:1549–1559
15. Kennedy AJ, Hull MS, Bednar AJ, Goss JD, Gunter JC, Bouldin JL, Vikesland PJ, Steevens JA (2010) Fractionating nanosilver: importance for determining toxicity to aquatic test organisms. *Environ Sci Technol* 44:9571–9577
16. Elzey S, Grassian VH (2010) Agglomeration, isolation and dissolution of commercially manufactured silver nanoparticles in aqueous environments. *J Nanoparticle Res* 12:1945–1958
17. Liu JY, Sonshine DA, Shervani S, Hurt RH (2010) Controlled release of biologically active silver from nanosilver surfaces. *ACS Nano* 4:6903–6913
18. Kittler S, Greulich C, Diendorf J, Koller M, Epple M (2010) Toxicity of silver nanoparticles increases during storage because of slow dissolution under release of silver ions. *Chem Mater* 22:4548–4554
19. Haase A, Arlinghaus HF, Tentschert J, Jungnickel H, Graf P, Manton A, Draude F, Galla S, Plendl J, Goetz ME, Masic A, Meier W, Thuenemann AF, Taubert A, Luch A (2011) Application of laser postionization secondary neutral mass spectrometry/time-of-flight secondary ion mass spectrometry in nanotoxicology: visualization of nanosilver in human macrophages and cellular responses. *ACS Nano* 5:3059–3068
20. MacCusprie RI, Allen AJ, Hackley VA (2011) Dispersion stabilization of silver nanoparticles in synthetic lung fluid studied under in situ conditions. *Nanotoxicology* 5:140–156
21. Stebounova L, Guio E, Grassian V (2011) Silver nanoparticles in simulated biological media: a study of aggregation, sedimentation, and dissolution. *J Nanoparticle Res* 13:233–244
22. MacCusprie RI (2011) Colloidal stability of silver nanoparticles in biologically relevant conditions. *J Nanoparticle Res* 13:2893–2908
23. Zook JM, MacCusprie RI, Locascio LE, Halter MD, Elliott JT (2011) Stable nanoparticle aggregates/agglomerates of different sizes and the effect of their size on hemolytic cytotoxicity. *Nanotoxicology*. doi:10.3109/17435390.17432010.17536615
24. Hackley VA, Clogston JD (2007) NIST-NCL joint assay protocol PCC-1: measuring the size of nanoparticles in aqueous media using batch-mode dynamic light scattering. Available at http://ncl.cancer.gov/working_assay-cascade.asp
25. ISO (1993) Guide to the expression of uncertainty in measurement, 1st edn. ISO, Geneva
26. USEPA (2002) Methods for measuring the acute toxicity of effluents and receiving waters to freshwater and marine organisms. 821/R-802-012. United States Environmental Protection Agency, Washington
27. Shaff JE, Schultz BA, Craft EJ, Clark RT, Kochian LV (2010) GEOCHEM-EZ: a chemical speciation program with greater power and flexibility. *Plant and Soil* 330:207–214
28. DECHEMA (1992) Handbook of corrosion. VCH Publishers, Weinheim
29. Tsai D-H, DelRio FW, Keene AM, Tyner KM, MacCusprie RI, Cho TJ, Zachariah MR, Hackley VA (2011) Adsorption and conformation of serum albumin protein on gold nanoparticles investigated using dimensional measurements and in situ spectroscopic methods. *Langmuir* 27:2464–2477
30. Tsai D-H, DelRio FW, MacCusprie RI, Cho TJ, Zachariah MR, Hackley VA (2010) Competitive adsorption of thiolated polyethylene glycol and mercaptopropionic acid on gold nanoparticles measured by physical characterization methods. *Langmuir* 26:10325–10333
31. Bland JM, Altman DG (1986) Statistical-methods for assessing agreement between 2 methods of clinical measurement. *Lancet* 1:307–310